Meiotic and epigenetic defects in Dnmt3L-knockout mouse spermatogenesis

Kylie E. Webster*†, Moira K. O'Bryan†‡, Stephen Fletcher§, Pauline E. Crewther*, Ulla Aapola¶, Jeff Craig‖, Dion K. Harrison§, Hnin Aung§, Nawapen Phutikanit§, Robert Lyle**, Sarah J. Meachem††, Stylianos E. Antonarakis**, David M. de Kretser‡, Mark P. Hedger‡, Pärt Peterson‡‡, Bernard J. Carroll§,§§, and Hamish S. Scott*¶¶

*Genetics and Bioinformatics Division, The Walter and Eliza Hall Institute of Medical Research, 1G Royal Parade, Parkville, Victoria 3050, Australia; ‡Centre for Molecular Reproduction and Endocrinology, Monash Institute of Reproduction and Development, Australian Research Council Centre of Excellence in Biotechnology and Development, Monash University, Clayton, Victoria 3168, Australia; §Schools of Molecular and Microbial Sciences and Land and Food Sciences and §§Australian Research Council Centre of Excellence for Integrative Legume Research and Institute of Molecular Bioscience, University of Queensland, Brisbane 4072, Australia; ¶Institute of Medical Technology and Department of Pathology, Biokatu 6, Tampere University Hospital, 33014 University of Tampere, Fin-33521, Tampere, Finland; ‖Chromosome Research Group, The Murdoch Children's Research Institute, Royal Children's Hospital, Flemington Road, Parkville, Victoria 3052, Australia; **Department of Genetic Medicine and Development, University of Geneva Medical School and University Hospitals of Geneva, CMU, 1, Rue Michel Servet, 1211 Geneva, Switzerland; ††Prince Henry's Institute of Medical Research, Monash Medical Centre, Clayton, Victoria 3168, Australia; and ‡‡Molecular Pathology, University of Tartu, Tartu 50414, Estonia

Communicated by Suzanne Cory, The Walter and Eliza Hall Institute of Medical Research, Parkville, Victoria, Australia, January 26, 2005 (received for review September 9, 2004)

The production of mature germ cells capable of generating totipotent zygotes is a highly specialized and sexually dimorphic process. The transition from diploid primordial germ cell to haploid spermatozoa requires genome-wide reprogramming of DNA methylation, stage- and testis-specific gene expression, mitotic and meiotic division, and the histone–protamine transition, all requiring unique epigenetic control. Dnmt3L, a DNA methyltransferase regulator, is expressed during gametogenesis, and its deletion results in sterility. We found that during spermatogenesis, Dnmt3L contributes to the acquisition of DNA methylation at paternally imprinted regions, unique nonpericentric heterochromatic sequences, and interspersed repeats, including autonomous transposable elements. We observed retrotransposition of an LTR-ERV1 element in the DNA from *Dnmt3L*$^{-/-}$ germ cells, presumably as a result of hypomethylation. Later in development, in *Dnmt3L*$^{-/-}$ meiotic spermatocytes, we detected abnormalities in the status of biochemical markers of heterochromatin, implying aberrant chromatin packaging. Coincidentally, homologous chromosomes fail to align and form synaptonemal complexes, spermatogenesis arrests, and spermatocytes are lost by apoptosis and sloughing. Because Dnmt3L expression is restricted to gonocytes, the presence of defects in later stages reveals a mechanism whereby early genome reprogramming is linked inextricably to changes in chromatin structure required for completion of spermatogenesis.

epigenetics | meiosis | histone modification | heterochromatin | DNA methylation

Chromatin modification is central to epigenetic control of the genome. Recently, mechanistic links between histone modifications, DNA methylation, and chromatin remodeling have emerged, giving clues to the interlocking layers of regulation that exist (1). Spermatogenesis has the unique epigenetic requirements of genomic imprint establishment, specialized transcription, meiosis, and the histone–protamine transition. Data on epigenetic modifications specific to gametogenesis is, however, mostly restricted to imprint establishment (2). The establishment of genomic imprints is defined by the sex-specific acquisition of differential methylation on a small subset of genes. Despite lacking methyltransferase activity (3, 4), DNA methyltransferase 3-like (Dnmt3L) is essential for the establishment of maternal methylation imprints during oogenesis (5, 6), probably by stimulation of Dnmt3a (7). Recent reports indicate that it has a similar role in the establishment of paternal imprints, although the extent to which it is required appears to vary between studies (7, 8). Progeny of *Dnmt3L*$^{-/-}$ females fail to develop past 9.5 d postcoitum, and *Dnmt3L*$^{-/-}$ males are sterile, with spermatocytes failing to complete meiosis (5, 6, 8). This divergence of phenotype is indicative of either a sex-specific Dnmt3L function or different developmental consequences in the absence of the same function. A male-specific function was supported by the finding that *Dnmt3L*$^{-/-}$ male germ cells also display hypomethylation at the long interspersed nuclear element (LINE)-1 and intracisternal A particle (IAP) transposons, indicating a wider role in *de novo* methylation (8).

The erasing and resetting of genomic imprints is part of a larger program of genome-wide reprogramming during gametogenesis. Despite this, little is known about the extent or functional consequences of DNA methylation at other single-copy or repeat sequences (9, 10). The rapid demethylation of the paternal genome (excluding imprinted regions) in the zygote (9, 11) suggests that the methylation at nonimprinted sequences may be reset specifically for successful passage through spermatogenesis.

Passage through spermatogenesis requires not only a unique program of transcription but also dynamic chromatin morphogenesis during meiosis and the histone–protamine transition. Meiosis differs substantially from mitosis in that it involves the exchange of genetic material between homologous chromosomes. This additional complexity requires further chromatin remodeling and transcriptional regulation, particularly during prophase I when chromosomes condense, seek out their homologs, align, synapse, and recombine (12–16). The mechanisms underlying mammalian homolog recognition and pairing are not well understood (17), and little is known about the epigenetic mechanisms regulating these steps.

Our analysis of *Dnmt3L*$^{-/-}$ males reveals direct roles for Dnmt3L in epigenetic changes that occur throughout the early stages of spermatogenesis. Dnmt3L contributes to the acquisition of DNA methylation not only at paternally imprinted regions but also at unique nonpericentric heterochromatic sequences and interspersed repeats. Chromatin compaction appears to be impaired in meiotic cells, as evidenced by differences in the accessibility of histone epitopes, and homologous chromosomes fail to align and form synaptonemal complexes (SCs), leading to spermatogenetic arrest and loss of spermatocytes. These results indicate that many of the specialized changes in

Freely available online through the PNAS open access option.

Abbreviations: AMP, amplified methylation polymorphism; IHC, immunohistochemistry; KO, knockout; SC, synaptonemal complex; DMR, differentially methylated region; LINE, long interspersed nuclear element.

†K.E.W. and M.K.O. contributed equally to this work.

¶¶To whom correspondence should be addressed. E-mail: hscott@wehi.edu.au.

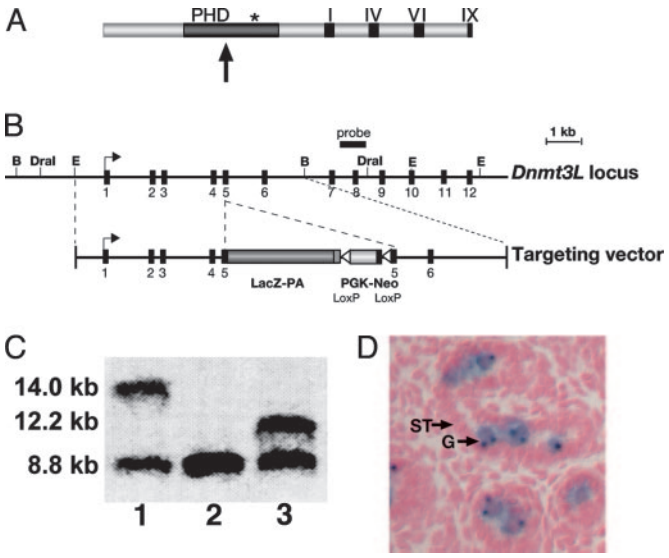

Fig. 1. Disruption of *Dnmt3L* and its expression in gonocytes. (*A*) The Dnmt3L protein, plant homeodomain (PHD)-like domain, nuclear localization signal (*), and C-terminal motifs (I, IV, VI, and IX) relative to the insertion site of the LacZ gene (arrow) (3). (*B*) Targeted disruption of *Dnmt3L*. E, *Eco*RI; B, *Bam*HI; PA, polyadenylation signal; PGK-Neo, phosphoglycerate kinase neomycin. (*C*) Southern blot analysis of *Dra*I-digested ES cell DNA (3′ probe) gave products of 8.8 kb (lane 2), 14.0 kb (lane 1), and 12.2 kb (lane 3) for the WT, targeted, and excised alleles, respectively. (*D*) LacZ reporter gene expression in gonocytes (G) of newborn testis. ST, seminiferous tubule.

chromatin morphology occurring during meiosis require Dnmt3L, either directly or indirectly.

Materials and Methods

For details, see *Supporting Materials and Methods*, which is published as supporting information on the PNAS web site.

***Dnmt3L* Targeting Vector and Generation of Knockout (KO) Mice.** *Dnmt3L* KO mice were generated by the insertion of the LacZ gene into exon 5, disrupting the plant homeodomain-like zinc finger domain (Fig. 1 *A* and *B*). The phosphoglycerate kinase-neomycin cassette was later removed by breeding the mice to a *cre*-transgenic strain (18). Southern blot analysis detected products of 8.8, 14.0, and 12.2 kb for the WT, targeted, and excised alleles, respectively (Fig. 1*C*).

X-Gal Staining. Tissues were embedded in Tissue-Tek OCT compound (Sakura Finetek, Torrance, CA) and snap-frozen in isopentane/liquid nitrogen. Cryostat sections (10 μm) were stained as described in ref. 19 and counterstained with nuclear fast red.

Testis TUNEL Staining and EM. Testes were fixed in Bouin's fluid and processed for histology (20). The timing of germ cell loss was determined by comparison of WT ($n = 8$), heterozygous (HET) ($n = 7$), and KO ($n = 8$) animals at ages indicative of the appearance of particular germ cell types: i.e., d 7, d 14, d 21, and $\geq$ d 35. The precise morphological abnormalities in spermatogenesis were determined by transmission EM (20) ($n = 2$, WT and KO). At least 30 spermatocytes from multiple fields were examined per animal. TUNEL staining was used to analyze apoptosis in WT ($n = 4$), HET ($n = 2$), and KO ($n = 3$) testes (Apotag Plus peroxidase, Intergen, Purchase, NY). All TUNEL-positive cells up to and including stage IV pachytene spermatocytes in all tubules in a cross section were counted. Only d 30–50 postnatal mice were included because of the bias caused by the progressive and rapidly degenerating seminiferous epithelium.

Immunohistochemistry (IHC). IHC was performed on Bouin's-fixed testes by using rabbit sera and the DAKO EnVision system as recommended by the manufacturer. Antibodies are listed in *Supporting Materials and Methods*.

Germ Cell Isolation. Centrifugal elutriation was used to separate spermatogenic cells into four size fractions (21): fraction II type B spermatogonia and preleptotene and leptotene spermatocytes for bisulfite genomic sequencing and fraction III type A and B spermatogonia were used for amplified methylation polymorphism (AMP) analysis. Contaminating somatic cells were $<10\%$. Isolations used WT (20 $\times$ postnatal d 10) and KO (14 $\times$ postnatal d 12–29) testes. This range of KO mice was used because of the general difficulties in obtaining age-matched juvenile mutant mice; however, the spermatocyte arrest in KO mice precluded any contamination from more mature cells. Two independent isolations were performed.

Bisulfite Genomic Sequencing. DNA was bisulfite-treated as described in ref. 22 (but with a 16-h incubation), PCR-amplified, subcloned, and sequenced.

AMP Protocol. Spermatogonia were analyzed for genome-wide methylation polymorphisms by using the AMP protocol (D.K.H., H.A., S.F., N.P., and B.J.C., unpublished data), described in more detail in *Supporting Materials and Methods*.

Results

Inactivation of *Dnmt3L* Causes Germ Cell Arrest in Meiotic Spermatocytes. To investigate the role of Dnmt3L, we analyzed its expression by using the LacZ reporter gene. X-Gal staining detected high levels of expression in the gonocytes of perinatal testes (Fig. 1*D*), as found previously (5). This expression was corroborated by using a Dnmt3L antibody (data not shown). Adult *Dnmt3L*$^{-/-}$ mice exhibited severe hypogonadism and were sterile. We first observed the appearance of germ cell aberrations early in meiosis of the first spermatogenic wave (d 14). At this time, the tubules appeared arrested, with many containing a buildup of leptotene and zygotene spermatocytes. However, germ cells with light microscopic characteristics of early pachytene spermatocytes (Fig. 2 *A* and *B*) were clearly visible (up to and including stage IV). Cell types beyond this stage of development were never observed. By d 70, however, only cells with a light microscopic appearance consistent with leptotene spermatocytes and spermatogonia were present, and the vast majority of tubules were Sertoli cell only (data not shown). TUNEL staining and transmission EM revealed that germ cells were lost both by apoptosis and germ cell sloughing into the tubule lumen, whereby entire clonal lines were ejected by Sertoli cells (Fig. 2 *C–F*). The number of TUNEL-positive cells per section of KO testes far exceeded that in WT sections (Fig. 2*I*). Because the apoptosis occurs on a background of increasing spermatogenic "dropout" by sloughing, the number of apoptotic cells counted in the TUNEL assay certainly underestimates the contribution of apoptosis to germ cell loss. The processes of apoptosis and sloughing were reflected in the "vacuolated" appearance of the epithelium (Fig. 2*F*). Sertoli cells retained normal Sertoli–Sertoli cell junctions, indicating that the progressive phenotype was not due to breakdown of the blood–testis barrier (Fig. 5, which is published as supporting information on the PNAS web site).

Male Germ Cell Arrest Results from Failure to Form the SC. By using transmission EM, abnormalities in *Dnmt3L*$^{-/-}$ testes were first detected in prophase I during the first spermatogenic wave.

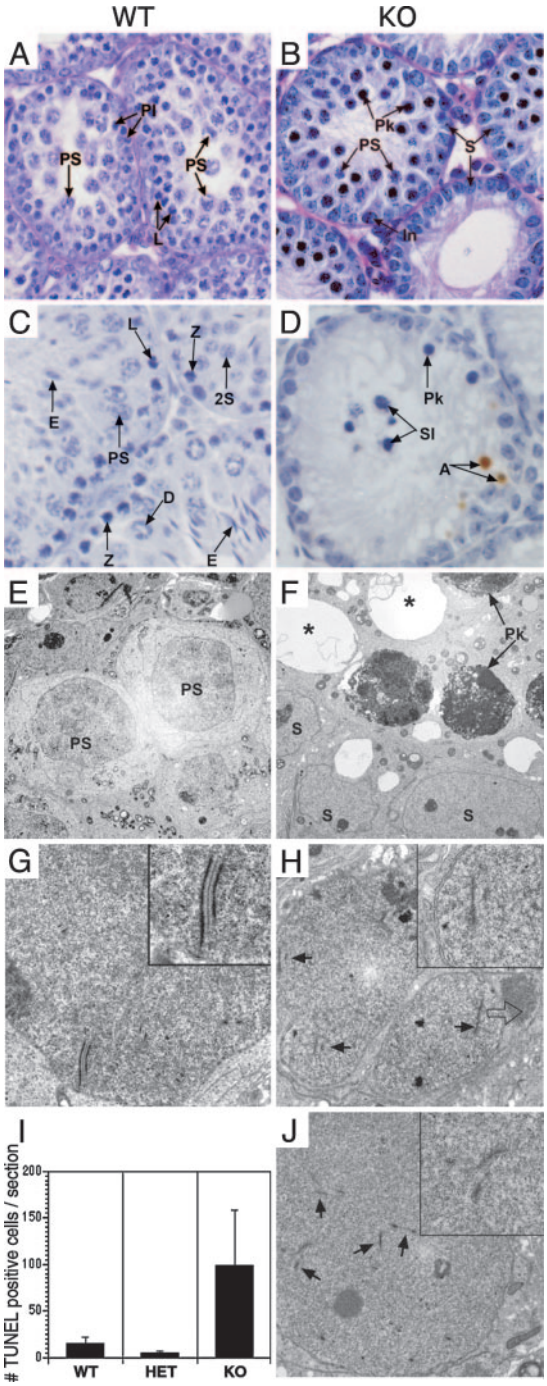

Fig. 2. *Dnmt3L*$^{-/-}$ germ cells are lost by sloughing and apoptosis after failure of homologous chromosome alignment and synapsis. WT (*A*, *C*, *E*, and *G*) and *Dnmt3L*$^{-/-}$ (KO) (*B*, *D*, *F*, *H*, and *J*) testes are shown. (*A*) WT d 14 testes. (*B*) KO d 14 testes containing cells with pyknotic nuclei (Pk) consistent with apoptosis and cells with characteristics of early pachytene spermatocytes (PS). (*C*) TUNEL staining of d 41 WT. (*D*) TUNEL staining of d 41 KO reveals an increase in apoptotic cells (A) (brown staining). Germ cell sloughing (Sl) was frequently observed. (*E*) EM of d 22 WT testes. (*F*) EM of d 22 KO testes shows many degenerating cells and vacuolation (*) indicative of recent germ cell loss. (*G*) The tripartite appearance of homologous chromosomes synapsed by means of the SC (*Inset*) in WT pachytene spermatocytes. (*H* and *J*) KO testes contained single unpaired chromosomes and partially paired chromosomes (arrows). Abnormal ribosomal clumps were frequently found (open arrow). (*I*) Graphical representation of the number of TUNEL-positive cells per section of WT, heterozygous, and KO testes. In, intermediate spermatogonia; E, elongating spermatid; S, Sertoli cell. Spermatocytes: Pl, preleptotene; L, leptotene; Z, zygotene; D, diplotene; 2S, secondary.

Single leptotene threads, indicative of unpaired condensed chromosomes, were detected in *Dnmt3L*$^{-/-}$ spermatocytes (Fig. 2*H*). Normally, synapsis of homologous chromosomes commences in zygotene and is completed by the pachytene stage (Fig. 2*G*). Although occasional profiles from *Dnmt3L*$^{-/-}$ testes suggested that partial synapsis had occurred, the central elements were poorly developed and barely visible (Fig. 2 *H* and *J*). The classical tripartite appearance of the pachytene SC was not observed (Fig. 2*G*). Furthermore, many leptotene spermatocytes showed abnormal aggregates of ribosomal particles (Fig. 2*H*) (also visible by light microscopy). These observations indicate that the cells identified at the light microscopic level during the first wave of spermatogenesis, with morphological characteristics consistent with zygotene and pachytene spermatocytes, were, in fact, ultrastructurally abnormal. This finding is consistent with the aberrant appearance of *Dnmt3L*$^{-/-}$ meiotic chromosome spreads stained with an antibody against the SC protein 3 (data not shown) (23). Asynapsis, nonhomologous synapsis, and complex branched structures were observed, with no spermatocytes achieving complete synapsis (pachytene), in agreement with a previous report (8).

Dnmt3L Is Required for Correct Establishment of Paternal Methylation Imprints. Because Dnmt3L is essential for the establishment of maternal methylation imprints during oogenesis (5, 6), we investigated the methylation status of imprinted genes in male germ cells by using bisulfite sequencing. We analyzed a cell preparation of type B spermatogonia, preleptotene, and leptotene spermatocytes, a population in which the methylation of paternal sequences should be nearing completion and all maternal imprints are erased (24). The differentially methylated regions (DMRs) of maternally imprinted genes *Snrpn* and *Igf2r* were appropriately unmethylated in KO mice (Fig. 6, which is published as supporting information on the PNAS web site), whereas the DMRs of *H19* and *Rasgrf1* displayed marked differences from control animals. In WT animals, the majority of alleles had acquired methylation (Fig. 3 *A* and *B*), with unmethylated alleles attributed to the variable maturity of the cell preparation and methylation normally continuing until pachytene spermatocytes (24). In contrast, the majority of alleles of the KO *Rasgrf1* DMR were unmethylated, and the *H19* DMR displayed a mosaic methylation pattern within strands (Fig. 3 *A* and *B*). This mosaic methylation of H19 confirms that reported recently (8), whereas the hypomethylation of Rasgrf1 differs from a previous finding (7). These results indicate that Dnmt3L is required for the establishment of normal paternal methylation imprints during spermatogenesis. However, the locus-specific effects and the presence of some methylation in *Dnmt3L*$^{-/-}$ male germ cells, but not *Dnmt3L*$^{-/-}$ female germ cells (5, 6), suggest sex-specific differences in the mechanism of Dnmt3L-mediated methylation during gametogenesis.

Dnmt3L Is Required for Methylation at Additional Genomic Sequences. It seemed unlikely that the abnormal methylation of imprinted genes could be responsible for such a profoundly disrupted meiotic phenotype. Moreover, because Dnmt3L can stimulate DNA methyltransferase activity in a sequence-independent manner (4), we were interested in the methylation status of other genomic regions. We applied the AMP protocol (D.K.H., H.A., S.F., N.P., and B.J.C., unpublished data) to compare the genome-wide methylation patterns of DNA from *Dnmt3L*$^{-/-}$ and WT spermatogonia. We compared ≈1,960 amplified loci or 3,920 CpG dinucleotide sites, representing ≈0.008% of the estimated 5×10^7 5-mCpG sites in the genome (25). From these 1,960 loci, we detected 22 methylation polymorphisms that showed loss of DNA methylation in *Dnmt3L*$^{-/-}$ spermatogonia (Fig. 3*C*; see also Fig. 7, which is published as supporting information on the PNAS web site), indicative of ≈1–2% of

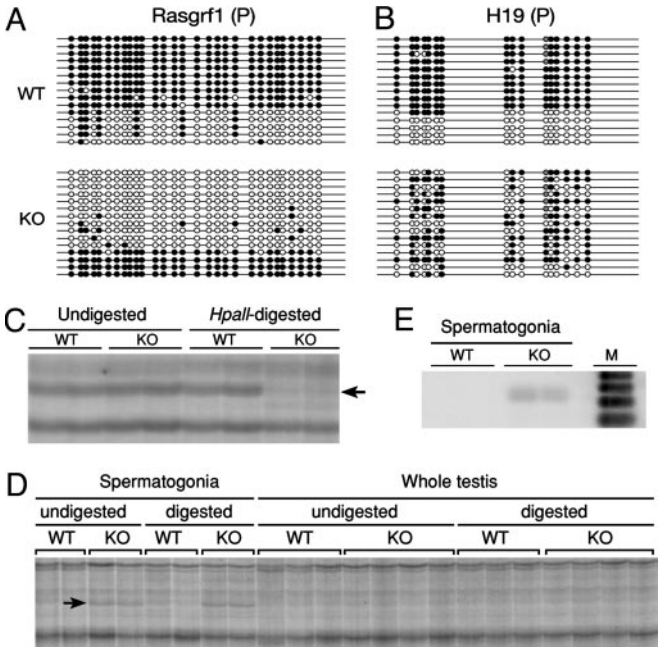

Fig. 3. Abnormal DNA methylation in *Dnmt3L*$^{-/-}$ germ cells. (*A* and *B*) Bisulfite genomic sequencing of *H19* and *Rasgrf1* paternally (P) imprinted loci from WT and KO germ cells. Each line corresponds to a single strand of DNA, and each circle represents an individual CpG dinucleotide. Filled circles, methylated CpG; open circles, unmethylated CpG; gray circles, incomplete sequence. (*C*) Portion of a gel showing an AMP-detected DNA methylation polymorphism in KO spermatogonia. Absence of the locus (arrow) only in digested KO DNA indicates loss of methylation. (*D*) Portion of the gel showing the AMP locus (arrow) detected in KO spermatogonia but not in WT spermatogonia or KO somatic cells. (*E*) Southern blot confirmation of the AMP locus shown in *D*. M, size marker.

normally methylated CpGs in the genome being hypomethylated. No PCR products coincided with the DMRs of *H19*, *Igf2r*, *Rasgrf1*, and *Snrpn*. We attempted to identify eight hypomethylated loci by cloning and sequencing and have confirmed the identity and sequence of three (Table 1). Among the confirmed loci, there are two LINEs (D2 and D4) and a unique GC-rich sequence (D3). Both D2 and D3 are in gene-poor heterochromatic regions of the genome, with D2 mapping to the X chromosome. D4 cannot be mapped precisely to the mouse genome, because its sequence is entirely contained within the 5′ UTR of the ≈7-kb or 5-kb consensus of either the L1Md_T or the L1Md_Gf subfamilies of L1s. This observation is consistent with a recent finding that showed hypomethylation and transcriptional activation of L1s in *Dnmt3L*$^{-/-}$ male germ cells (8). The cloning of the other five hypomethylated loci sometimes resulted in multiple clones and sequences from the same band. However, they could not be confirmed because of a lack of DNA. Despite this, the sequences obtained include other interspersed repeats, such as LTRs and short interspersed nuclear elements, and GC-rich regions but nothing that can be classified as a CpG island (data not shown). The involvement of Dnmt3L in the methylation of both imprinted regions and many other sequences, as detected by AMP, reveals a broad role for this protein in genome reprogramming during spermatogenesis.

In addition to the 22 hypomethylated loci, we identified a locus present in both the undigested and digested KO germ cell samples that was absent from the KO somatic cell aliquot and all WT germ cells (Fig. 3*D*). This identification indicates that we have detected a locus specific to the KO germ cells and thus a *de novo* mutation. We cloned, sequenced, and confirmed this locus (D1 in Table 1, and Fig. 3*E*). As with D4, D1 cannot be mapped precisely to the mouse genome, because its sequence is entirely contained within the 5′ UTR of the ≈7.5-kb consensus of the RLTR6_Mm-int subfamily of ERV1 LTRs. We conclude that the presence of this AMP band in germ cells, but not in somatic tissues of the *Dnmt3L*$^{-/-}$ mice, is due to retrotransposition.

Change in Chromatin Structure During Condensation and Synapsis in *Dnmt3L*$^{-/-}$ Meiotic Cells. The DNA methylation defects we observed appear to be a direct consequence of the absence of Dnmt3L during early spermatogenesis. However, because the spermatogenic crisis is not observed until early meiosis, we investigated the possibility of additional epigenetic anomalies that could link the early *Dnmt3L* expression and DNA methylation defects with the meiotic defect occurring cell divisions later. We examined the status of chromatin by IHC using a panel of antibodies against modified histones in WT and *Dnmt3L*$^{-/-}$ spermatogenic cells. Distinctive temporal differences in chromatin staining patterns were observed in WT and KO germ cells throughout the spermatogenic wave, using antibodies specific for acetylated and methylated histones (Fig. 4; see also Figs. 8 and 9, which are published as supporting information on the PNAS web site).

During WT spermatogenesis, spermatogonia through to preleptotene spermatocytes stained positively for acetylated histone H4 (associated with active, open euchromatin), whereas meiotic spermatocytes and round spermatids were negative. Acetylated histone H4 labeling was again detected in elongating spermatids (Fig. 4*A*) (26). Conversely, in the KO, acetylated H4 was observed in later stages, in cells with light microscopic characteristics of leptotene, zygotene, and early pachytene spermatocytes (the most mature stage observed) (Fig. 4*B*). This

Table 1. Differentially methylated loci in Dnmt3L KO germ cells

		U		H		Regions of highest homology		Proximity to repeat sequences				Proximity to gene sequence		
Name	Primer	WT	KO	WT	KO	Chromosome (strand)	Nucleotide position in genome	Proximity to repeat	Name	Family	Class	Proximity to gene	Nearest cds or gene	Likely target
D1	BB18	−	+	−	+	Y (−)	39319223–39319675	Overlapping	RLTR6_Mm-int	ERV1	LTR	213,375 bp 5′	NM_023546	LTR
						Y (−)	24375709–24376056	Overlapping	RLTR6_Mm-int	ERV1	LTR	38,991 bp 3′	U16670	
						Y (−)	18390020–18390365	Overlapping	RLTR6_Mm-int	ERV1	LTR	584,560 bp 5′	AK017055	
D2	AE11	−	−	−	+	X (−)	132160393–132160530	Overlapping	Lx2B	L1	LINE	29,583 bp 3′	NM 172782	LINE
D3	V15	+	+	+	−	12 (+)	101033492–101033755	3,180 bp 3′	MIRb	MIR	SINE	223,016 bp 3′	AK038308	GC rich
D4	AE11	−	−	−	+	10 (+)	10283320–10283760	Overlapping	L1Md_T	L1	LINE	266 bp 3′	AK045941	LINE
						1 (+)	48600158–48600388	Overlapping	L1Md_Gf	L1	LINE	266 bp 3′	AK045941	
						X (−)	33831816–33832045	Overlapping	L1Md_T	L1	LINE	Overlap intron	NM_016886	

SINE, short interspersed nuclear element; U, undigested spermatogonia DNA; H, *Hpa* II-digested spermatogonia DNA; cds, coding sequence.

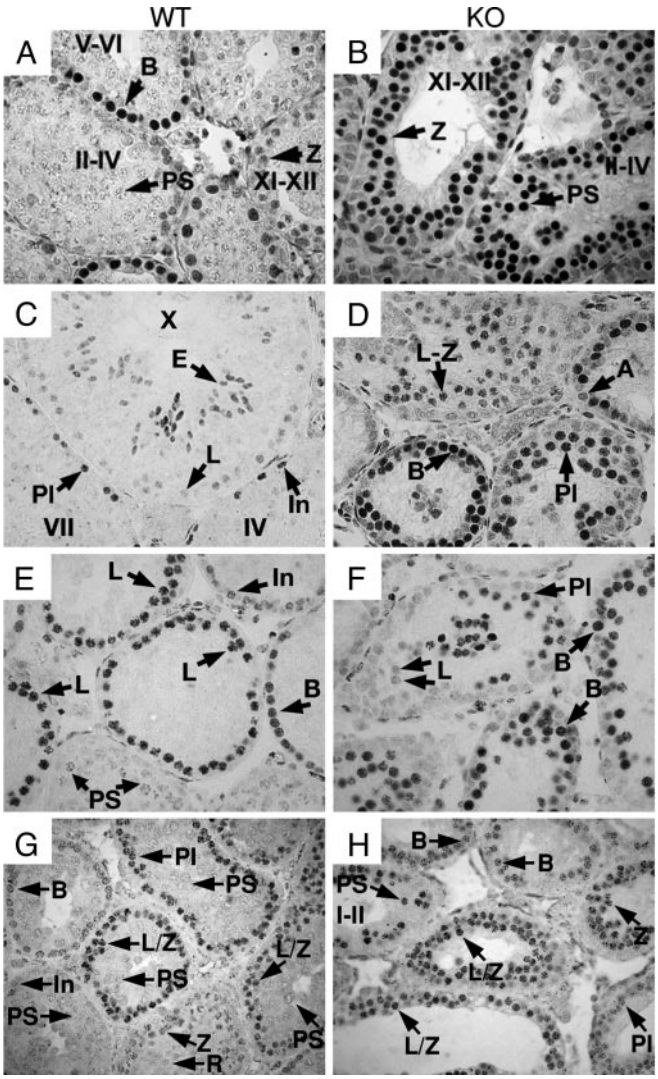

Fig. 4. Differential detection of histone modifications in *Dnmt3L*$^{-/-}$ germ cells. (*A* and *B*) Acetylated H4 was detected in leptotene (L), zygotene (Z), and pachytene (PS) spermatocytes in KO (*B*) but not in WT (*A*) testes at all ages (d 21 shown). (*C* and *D*) Acetylated H3K9 was detected in leptotene and zygotene spermatocytes in KO (*D*) but not in WT (*C*) adult testes (d 42). (*E* and *F*) Dimethylated H3K9 was detected in leptotene and zygotene spermatocytes in WT (*E*) but not in KO (*F*) testes at all ages (d 21 shown). (*G* and *H*) Unmodified histone H3 stained strongly in pachytene spermatocytes of KO (*H*) but not WT (*G*) testes. Spermatogonia: In, intermediate; A, type A; B, type B; Pl, preleptotene spermatocyte; R, round spermatid; E, elongating spermatid. Roman numerals indicate seminiferous tubule stage.

observation was verified by using three antibodies (Figs. 8 and 9). Furthermore, during the first wave of spermatogenesis in WT mice, cells from the intermediate spermatogonia stage through the zygotene spermatocyte stage stained positively for another epigenetic marker of euchromatin, histone H3 acetylated at lysine 9 (acetyl H3K9). In subsequent spermatogenic waves (i.e., adult tissue), staining for acetyl H3K9 was seen only in cells from the spermatogonia stage through to the preleptotene spermatocytes stage (inclusive) (Fig. 4*C*). As with acetylated H4, staining for acetyl H3K9 extended to later stages of meiotic prophase in KO germ cells, from intermediate spermatogonia through to zygotene spermatocytes, in both the first and subsequent waves of spermatogenesis (Fig. 4*D*).

Although euchromatin-specific histone modifications were aberrantly maintained through the leptotene, zygotene, and pachytene stages in KO cells, the opposite was observed for dimethyl H3K9, an epigenetic marker of inactive, condensed heterochromatin. Staining for dimethyl H3K9 was observed in type B spermatogonia to zygotene spermatocytes in WT mice (Fig. 4*E*), but in KO germ cells, staining was restricted to type B spermatogonia and preleptotene spermatocytes (Fig. 4*F*). However, staining for trimethyl H3K9, a marker for pericentric heterochromatin, did not diverge from WT patterns and was positive from type B spermatogonia onward (data not shown).

We observe here a shift from a heterochromatic state to a euchromatic state in *Dnmt3L*$^{-/-}$ germ cells between leptonema and pachynema. Interestingly, using the same antibodies, almost all epitopes could be detected in both KO and WT mice at all stages in meiotic chromosome spreads (Fig. 10, which is published as supporting information on the PNAS web site). We suggest that the change from heterochromatin to euchromatin in *Dnmt3L*$^{-/-}$ germ cells loosens chromatin structure to permit some antibodies increased access to their epitopes. Because chromosomes in chromosome spreads are subjected to a lesser degree of aldehyde-mediated protein cross-linking compared with those fixed *in situ* by Bouin's fixative, they are likely to exhibit greater antigen accessibility (27), effectively eradicating any differences observed *in situ*. In support of this interpretation, we found by using IHC that an antibody to unmodified histone H3 showed stronger staining of pachytene spermatocytes in KO compared with WT testis sections (Fig. 4 *G* and *H*).

Discussion

Chromatin structure is central to the epigenetic processes controlling the function and stability of genomes in eukaryotic organisms from yeast to mammals. Here we show that during mouse spermatogenesis, Dnmt3L activity affects DNA methylation not only at paternally imprinted regions but also at other sequences, including unique nonpericentric heterochromatic sequences and interspersed repeats. Later, after at least three cell divisions (28) and differentiation into meiotic spermatocytes, chromatin compaction appears to be affected, as indicated by differences in the accessibility of histone epitopes by IHC. This loss of chromatin compaction coincides with poorly aligned and unpaired chromosomes in zygotene and pachytene spermatocytes, which are known to trigger the pachytene checkpoint (29), leading to germ cell arrest and apoptosis, as we observed. Furthermore, the germ cell sloughing suggests that the presence of defective spermatocytes may have disturbed paracrine communications with the Sertoli cells (30), leading to the release of entire clonal lines into the tubule lumen and, consequently, progressive degeneration of the seminiferous epithelium to a Sertoli cell-only phenotype.

The presence of defects in DNA methylation at both imprinted regions and other sequences in *Dnmt3L*$^{-/-}$ cells provides insight into male genome reprogramming. Although some differentially methylated AMP loci are unique nonrepetitive sequences, they often fall within and/or contain repetitive DNA (H.A., H.S.S., and B.J.C., unpublished data). From four confirmed AMPs in this study, we identified two LINEs, one LTR, and one unique sequence. One of the LINEs and the LTR belong to subfamilies of full-length elements known to be capable of active retrotransposition. The mapping of AMP loci to transposons is consistent with the demonstrated role of Dnmt3L-mediated DNA methylation in the transcriptional silencing of these autonomous LINE and LTR transposable elements during spermatogenesis (8). Also, the presence of an AMP band in KO germ cells, but not in somatic tissues, indicates that the retrotransposition of a LTR-ERV1 element in the KO germ cell DNA had occurred. This retrotransposition probably results from transcriptional reactivation of a RLTR6_Mm-int-ERV1 retroviral element due to hypomethylation, subsequent reverse transcription, and reintegration, resulting in a *de novo* mutation in the germ cells.

Although it is not possible to say from where in the mouse genome the retrotransposed element was derived, the top three sites' BLAT matches were all from the Y chromosome (Table 1), and, of only 73 sites in the genome with a >98.5% homology to the cloned AMP, 11 and 13 were from the Y and X chromosomes, respectively. Thus, Dnmt3L is involved in methylation of imprinted regions, some interpersed repeats, and other unique nonpericentric heterochromatic sequences. This finding indicates that during male genome reprogramming, in contrast with female genome reprogramming (5), the methylation of imprinted genes is integrated into a larger program of methylation involving Dnmt3L. Because Dnmt3L can stimulate DNA methylation independent of sequence (4, 31), these sequences may be targeted because of some other shared epigenetic form.

In addition to the DNA hypomethylation detected in *Dnmt3L*$^{-/-}$ spermatogonia, differences in detection of various histone tail epitopes and core H3 histone were observed by IHC in meiotic cells. Differences were found at acetyl groups on histones H3 and H4 and dimethyl groups on histone H3 (Figs. 4, 8, and 9). These differences flagged a change of chromatin structure on chromosome arms from a heterochromatic state to a euchromatic state. That this shift in chromatin state is accompanied by a change in general chromatin accessibility was confirmed by the differences observed with core H3 histone antiserum. Despite this, it is difficult to say from our results whether there is also a quantitative difference in the modification of the various histone tail epitopes in KO and WT mice, as opposed to simply a change in epitope accessibility. Nonetheless, a defect in forming compact heterochromatin is likely to be the underlying cause of the failure of chromosome alignment in meiotic spermatocytes.

Heterochromatin is found in large blocks surrounding centromeres and telomeres and is concentrated in smaller domains interspersed throughout the chromosome (32). Hypomethylation of sequences in nonpericentric heterochromatic regions (D2 and D3 in Table 1), in addition to abnormalities in dimethyl and not trimethyl H3K9 antigen accessibility in KO spermatocytes, implies that formation of interspersed heterochromatic regions, and not pericentric or centromeric heterochromatic regions (33), are defective in *Dnmt3L*$^{-/-}$ meiotic chromosomes. This observation is supported by the recent finding that interspersed autonomous LINE and LTR sequences, but not pericentric repeat sequences, are demethylated in *Dnmt3L*$^{-/-}$ male germ cells (8). In spermatocytes, compaction of nonpericentromeric heterochromatin could prevent the participation of ubiquitously distributed repetitive sequences in the homology search (13) or, conversely, promote homolog recognition through the arrangement of heterochromatic sequences and associated proteins (34).

Because Dnmt3L expression is restricted to gonocytes, it does not seem possible that it could directly influence changes in chromatin conformation later in spermatocytes. Instead, it appears that Dnmt3L-mediated DNA methylation in gonocytes influences molecular interactions important for future chromatin compaction in the same way that DNA methylation during embryogenesis precedes histone modifications and is important in setting up the structural profile of chromatin during development (35).

Note. While this work was under consideration, two related articles were published (7, 8).

The LacZ-LoxP-Neo-PGK-LoxP cassette was a gift from Yann Herault and Denis Duboule (University of Geneva). We thank Edouard G. Stanley and members of the Mouse Genome Manipulation Services at The Walter and Eliza Hall Institute of Medical Research (WEHI); Loretta Gibson, Ping Cannon, Lavinia Hyde, Amanda Eddy, Gabrielle Douglas, and Julie Muir for excellent technical assistance; Huiling Xu for valuable discussions; Christa Heyting (Wageningen Agricultural University, Wageningen, The Netherlands) for antiserum to Scp3; WEHI Animal Services for animal care and management; and members of the H.S.S. laboratory for discussion. DNA sequencing was performed by the Australian Genome Research Facility, established through the Commonwealth-funded Major National Research Facilities Program. This work was supported by an Australian Postgraduate Award (to K.E.W.); National Health and Medical Research Council (NHMRC) Fellowships 143781 (to M.K.O.), 143788 (to M.P.H.), and 171601 (to H.S.S.); NHMRC Program Grants 257501 (to H.S.S.) and 143786 (to M.K.O., M.P.H., and D.D.K.); the Nossal Leadership Award from WEHI (to H.S.S.); an Australian Research Council Centre of Excellence grant (to M.K.O. and D.D.K.); and grants from the Swiss Fonds National Suisse de la Recherche Scientifique, the European Union/Office Fédéral de l'Education et de la Santé, the ChildCare Foundation, the National Center for Competence in Research-Frontiers in Genetics (to S.E.A.), the Medical Research Fund of Tampere University Hospital (to U.A. and P.P.), the Finnish Cultural Foundation (to U.A.), the Academy of Finland Sigrid Juselius Foundation, and the Wellcome Trust (to P.P.).

1. Li, E. (2002) *Nat. Rev. Genet.* **3,** 662–673.
2. Surani, M. A. (2001) *Nature* **414,** 122–128.
3. Aapola, U., Lyle, R., Krohn, K., Antonarakis, S. E. & Peterson, P. (2001) *Cytogenet. Cell Genet.* **92,** 122–126.
4. Chedin, F., Lieber, M. R. & Hsieh, C. L. (2002) *Proc. Natl. Acad. Sci. USA* **99,** 16916–16921.
5. Bourc'his, D., Xu, G. L., Lin, C. S., Bollman, B. & Bestor, T. H. (2001) *Science* **294,** 2536–2539.
6. Hata, K., Okano, M., Lei, H. & Li, E. (2002) *Development (Cambridge, U.K.)* **129,** 1983–1993.
7. Kaneda, M., Okano, M., Hata, K., Sado, T., Tsujimoto, N., Li, E. & Sasaki, H. (2004) *Nature* **429,** 900–903.
8. Bourc'his, D. & Bestor, T. H. (2004) *Nature* **431,** 96–99.
9. Reik, W., Dean, W. & Walter, J. (2001) *Science* **293,** 1089–1093.
10. Marchal, R., Chicheportiche, A., Dutrillaux, B. & Bernardino-Sgherri, J. (2004) *Cytogenet. Genome Res.* **105,** 316–324.
11. Oswald, J., Engemann, S., Lane, N., Mayer, W., Olek, A., Fundele, R., Dean, W., Reik, W. & Walter, J. (2000) *Curr. Biol.* **10,** 475–478.
12. Sybenga, J. (1999) *Chromosoma* **108,** 209–219.
13. Scherthan, H., Eils, R., Trelles-Sticken, E., Dietzel, S., Cremer, T., Walt, H. & Jauch, A. (1998) *J. Cell Sci.* **111,** 2337–2351.
14. Cook, P. R. (1997) *J. Cell Sci.* **110,** 1033–1040.
15. Page, S. L. & Hawley, R. S. (2003) *Science* **301,** 785–789.
16. Zickler, D. & Kleckner, N. (1999) *Annu. Rev. Genet.* **33,** 603–754.
17. McKee, B. D. (2004) *Biochim. Biophys. Acta* **1677,** 165–180.
18. Schwenk, F., Baron, U. & Rajewsky, K. (1995) *Nucleic Acids Res.* **23,** 5080–5081.
19. Luckett, J. C., Huser, M. B., Giagtzoglou, N., Brown, J. E. & Pritchard, C. A. (2000) *Cell Growth Differ.* **11,** 163–171.
20. Dickins, R. A., Frew, I. J., House, C. M., O'Bryan, M. K., Holloway, A. J., Haviv, I., Traficante, N., de Kretser, D. M. & Bowtell, D. D. (2002) *Mol. Cell. Biol.* **22,** 2294–2303.
21. Bucci, L. R., Brock, W. A., Johnson, T. S. & Meistrich, M. L. (1986) *Biol. Reprod.* **34,** 195–206.
22. Millar, D. S., Warnecke, P. M., Melki, J. R. & Clark, S. J. (2002) *Methods* **27,** 108–113.
23. Lammers, J. H., Offenberg, H. H., van Aalderen, M., Vink, A. C., Dietrich, A. J. & Heyting, C. (1994) *Mol. Cell. Biol.* **14,** 1137–1146.
24. Davis, T. L., Yang, G. J., McCarrey, J. R. & Bartolomei, M. S. (2000) *Hum. Mol. Genet.* **9,** 2885–2894.
25. Leonhardt, H. & Bestor, T. H. (1993) *EXS* **64,** 109–119.
26. Hazzouri, M., Pivot-Pajot, C., Faure, A. K., Usson, Y., Pelletier, R., Sele, B., Khochbin, S. & Rousseaux, S. (2000) *Eur. J. Cell Biol.* **79,** 950–960.
27. Peters, A. H., Plug, A. W., van Vugt, M. J. & de Boer, P. (1997) *Chromosome Res.* **5,** 66–68.
28. Tegelenbosch, R. A. & de Rooij, D. G. (1993) *Mutat. Res.* **290,** 193–200.
29. Nicklas, R. B., Ward, S. C. & Gorbsky, G. J. (1995) *J. Cell Biol.* **130,** 929–939.
30. de Kretser, D. M., Loveland, K. L., Meinhardt, A., Simorangkir, D. & Wreford, N. (1998) *Hum. Reprod.* **13,** Suppl. 1, 1–8.
31. Suetake, I., Shinozaki, F., Miyagawa, J., Takeshima, H. & Tajima, S. (2004) *J. Biol. Chem.* **279,** 27816–27823.
32. Grewal, S. I. & Elgin, S. C. (2002) *Curr. Opin. Genet. Dev.* **12,** 178–187.
33. Rice, J. C., Briggs, S. D., Ueberheide, B., Barber, C. M., Shabanowitz, J., Hunt, D. F., Shinkai, Y. & Allis, C. D. (2003) *Mol. Cell* **12,** 1591–1598.
34. Karpen, G. H., Le, M. H. & Le, H. (1996) *Science* **273,** 118–122.
35. Hashimshony, T., Zhang, J., Keshet, I., Bustin, M. & Cedar, H. (2003) *Nat. Genet.* **34,** 187–192.